Characterization of phosphorescence oxygen sensor based on erythrosin B in sol–gel silica in wide pressure and temperature ranges

S.K. Lam, M.A. Chan, D. Lo[*]

Physics Department, Chinese University of Hong Kong, Shatin, N.T., Hong Kong

Abstract

Room temperature phosphorescence emission of erythrosin B in sol–gel silica is studied over the oxygen pressure range from 10^{-6} to 1000 mbar. Quenching by oxygen is significant over the entire range. The Stern–Volmer (SV) intensity data can be very well fitted using the two-site model. The temperature dependence of the phosphorescence and the delayed fluorescence are examined from -173 to $200°C$ at an oxygen pressure of 0.015 mbar. The phosphorescence and delayed fluorescence show opposite trends of temperature dependence, which can be exploited for temperature compensation of the sensor probe. © 2001 Elsevier Science B.V. All rights reserved.

Keywords: Oxygen sensor; Fiber optic; Erythrosin B; Sol–gel; Silica

1. Introduction

Optical oxygen sensor based on luminescence quenching of molecular oxygen has received considerable interest in recent years. Most optical oxygen sensors in the literature are based on fluorescence quenching of the fluorophore, such as transition-metal complexes (e.g. ruthenium(II) (Ru(II) complexes), embedded in polymer or in sol–gel matrices [1–9]. These sensors are susceptible to several limitations: short lifetime (ns to μs range) [4], low sensitivity (fluorescence intensity variation less than 10 times between an oxygen concentration of 0–100%) [2]. High-speed and high-sensitivity opto-electronics are, therefore, needed for signal processing, adding cost and technical complexity to the oxygen sensing system.

An alternative approach to fluorescence sensing is phosphorescence sensing [10,11]. By virtue of the superior spectroscopic properties of phosphorescence (e.g. long lifetime, delayed emission, large separation of the absorption and emission peaks), phosphorescence based oxygen sensors promise higher sensitivity than fluorescence based oxygen sensors.

We have studied the delayed luminescence emissions of many dyes in sol–gel silica [12,13]. Recently we reported a fiber-optic oxygen sensor based on erythrosin B trapped in sol–gel silica which has a phosphorescence quantum yield of 2%. The Stern–Volmer (SV) ratio (the ratio of the luminescence intensity in vacuum and that in atmospheric oxygen pressure) is higher than 100 [14]. Because of the high porosity of the sol–gel matrix, the response time of this sensor can be estimated to be ∼100 ms, but can be reduced to less than 10 ms with a solenoid valve [14]. The phosphorescence oxygen sensor has been characterized over a limited oxygen pressure range and at two different temperatures [13]. To meet the application requirements that spring from biological/clinical monitoring to the automobile industry, complete characterization over wide operation range is clearly needed.

As in many luminescence-based oxygen sensors [1–11], the SV quenching plot of the phosphorescence data exhibits a nonlinear, negatively deviating behavior. The cause for this non-linear behavior is usually ascribed to the microheterogeneity of the local environment of the dye molecules in the host matrix. In actual experiments, the downward I_0/I plots pose difficulty for accurate calibration. Re-calibration of the sensors is often necessary prior to measurements. The number of calibration points required depends on the form of the calibration function. In this paper, we examined the oxygen quenching effect of our phosphorescence oxygen sensor over a wide oxygen pressure (P_{O_2}) range (10^{-6}–10^3 mbar). Several models were used to fit the non-linear SV intensity plots so that a fitting routine that can provide the most convenient and accurate calibration procedure can be determined.

---

[*] Corresponding author. Tel.: +852-2609-6103; fax: +852-2603-5204.
E-mail address: dlo@phy.cuhk.edu.hk (D. Lo).

Another problem faced by most fluorescent oxygen sensors is the temperature dependence. Luminescence based oxygen sensors are sensitive to oxygen as well as to temperature [15]. The trends in oxygen and temperature sensitivity are often rather similar. This introduces complications in applications where temperature variation is significant. Erythrosin-B doped sol–gel sensor exhibits phosphorescence and delayed fluorescence emissions that have opposite temperature dependence [12,13]. This difference in temperature dependence can be exploited for calibration purpose. The phosphorescence intensity and the delayed fluorescence intensity are studied over a wide range of temperature and P_{O_2} in this work. By exploring the opposite trends of temperature dependence of the phosphorescence oxygen sensor, a self-contained temperature compensation scheme is proposed for our oxygen sensor.

2. Experimental

2.1. Chemicals

An amount of 0.1 M aqueous solution of NaOH was obtained by dissolving analytical grade of NaOH in deionized water. Tetramethoxysilance (TMOS) (99%) (Aldrich), erythrosin B (Aldrich) and analytical grade of methanol (Riedel-dehaën) were used. High purity oxygen gas was obtained from Hong Kong Oxygen Co. Ltd.

2.2. Preparation of the O_2 probe

Details of the sol–gel process can be found in [12]. In brief, tetramethoxysilane (TMOS), methanol, deionized water and NaOH were mixed under magnetic stirring at room temperature. The erythrosin B dye was added to the mixture and the resulting solution (sol) was casted in acrylic cuvettes, which were sealed with sticky tapes. The concentration of the erythrosin B in starting solution was 1×10^{-5} mol/l. The sol gelled within 10 min at room temperature. The gels were allowed to further dry, shrink and age at room temperature. After 2 weeks the gels were baked at 200°C for 24 h. The typical silica gels measured at 6 mm × 6 mm × 12 mm. The ends of a multi-mode optical fiber were soaked in methylene chloride for 1 min. The jacket and the cladding of the fibers were then removed mechanically. Subsequently, the cleaved fiber end was bonded to the silica gel surface using poly(methyl methacrylate) (PMMA) toluene solution as adhesive.

2.3. Instrumentation

All measurements were conducted in a stainless steel vacuum chamber evacuated by a diffusion-rotary pumping unit. Details of the schematic diagram of the experimental set-up can be found in [14]. All the oxygen probes were degassed in vacuum ($\sim 4 \times 10^{-6}$ mbar) for 1 day before measurements were taken. The 5 ns (full width at half maximum, FWHM) laser pulses of the second harmonic ($\lambda = 532$ nm) of a Nd:YAG laser were used as excitation source and were launched into the optical fiber bonded onto the sol–gel silica bulk surface. Luminescence of the oxygen probe was collected by the same fiber coupled to a fiber bundle, which was connected to a 0.3 m grating monochromator. A gatable intensified charge coupled device (ICCD) was used to collect the emission spectra. In order to measure only the phosphorescence spectra, the delay time (the time between the onset of the laser pulse and the onset of the gate pulse which was used to switch on the ICCD for light collection) was set to 70 ns and the gate width (exposure time of the ICCD) to 80 ms. The 70 ns delay time is longer than the decay time of fluorescence but much shorter than the decay times of phosphorescence. The influence of fluorescence is, therefore, screened off. Also, the gate width was set to 80 ms to allow time-integration of the entire phosphorescence and delayed fluorescence signals.

To study temperature stability of the oxygen probe, a freestanding erythrosin B doped silica gel, unattached to fiber, was used to avoid degradation of the PMMA adhesive during heating process. The silica gel was placed on a sample stage which was in contact with a cool finger and a filament heater such that it could be cooled/heated to an arbitrary temperature ranging from −173 to 200°C. Experiments were conducted at ambient pressure of 0.015 mbar for the temperature dependence measurements.

3. Results and discussion

3.1. Pressure dependence

Delayed luminescence spectra of the oxygen probe at various ambient oxygen pressures are shown in Fig. 1. Measurements were conducted at room temperature. The intensity of phosphorescence drops by approximately a factor of 3.6 as the oxygen pressure increases from vacuum ($\sim 4 \times 10^{-6}$ mbar) to 0.051 mbar. The SV ratio is calculated by taking the intensity of phosphorescence peak at vacuum as I_0. Contribution of delayed fluorescence at the peak position of the phosphorescence is removed in the calculation of the SV ratio to yield a result of higher accuracy. In practice, the contribution of delayed fluorescence is about 2%. The SV ratio at oxygen pressure of 1000 mbar is found to be ~ 123. This ratio is much higher than most of the oxygen probes reported in the literature (Table 1). This indicates that the quenching of room temperature phosphorescence of erythrosin B by oxygen is extremely effective. Sensitivity of the oxygen probe is sometimes defined as the partial oxygen pressure/concentration at which the luminescence intensity is equal to $I_0/2$ [16]. The sensitivity of our oxygen probe is found to be ~ 0.012 mbar (or $\sim 9 \times 10^{-3}$ Torr). Comparing with the other types of oxygen probes (Table 1), the sensitivity of oxygen probe based on

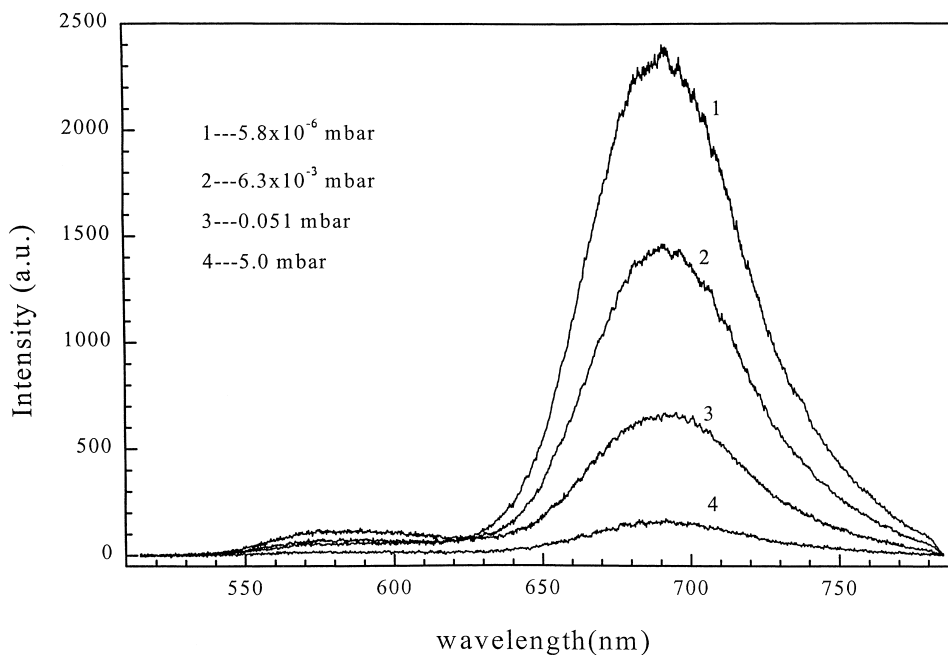Fig. 1. Phosphorescence and delayed fluorescence spectra of oxygen of erythrosin B in sol–gel at 5.8×10^{-6}, 6.3×10^{-3}, 0.051 and 5 mbar of oxygen pressure, respectively.

erythrosin B doped sol–gel silica is two orders of magnitude higher. Such high sensitivity is believed to be due to efficient phosphorescence quenching of erythrosin B and the very high porosity of the sol–gel derived silica matrix.

In Fig. 2, the SV ratio of the phosphorescence is plotted against the oxygen pressure in logarithmic scale. For the purpose of comparison with other sensors in the literature, a linear plot of the same SV curve of oxygen probe is inserted at the upper left corner of Fig. 2. The SV curve shows a typical non-linear dependence on oxygen pressure. Such non-linear SV curve is commonly observed in the lumines-cence quenching of luminophore immobilized in solid matrix. A number of models have been proposed to interpret the non-linear behavior of SV curves as a function of oxygen pressure [8,17–20,23–26]. Since most models require more than one variable parameter to describe the non-linear quenching response, several measurement points are needed for calibration, leading to added complexity of the calibra-tion process. For simplicity, the two-site model is often chosen to fit the non-linear SV plot. The two-site model [17–19] suggests that there are two different quenching sites

in the sensor with each quenching site obeying the linear SV equation and, hence, also its own quenching constant. The SV equation of the two-site model is written as

$$\frac{I_0}{I} = \frac{1}{f/(1 + K_1 P_{O_2}) + (1 - f)/(1 + K_2 P_{O_2})}$$

where I_0 and I are the intensities of the phosphorescence in the absence and presence of oxygen, respectively, K_1 and K_2 the quenching constants of two different sites, respectively, f the fraction of the sites with K_1 constant and P_{O_2} is the oxygen pressure. In Fig. 2, the solid line (two-site model) provides an excellent fit for the intensity-quenching curve over the full range of pressure covering nine orders of magnitude. The fitting parameters are listed in Table 2. The Gaussian [20,21] and the log-Gaussian [8,22] models have been examined for fitting the SV plot. Both models generate good fit at high (>10 mbar) and low ($<10^{-3}$ mbar) pressures. The good fit at high pressures are consistent with results reported in the literature [5–8,11]. In the intermediate pressure range (10^{-3}–10 mbar), however, predictions from both models seem to stray from the measurements.

Table 1
Properties of typical oxygen sensors[a]

Luminophore	I_0/I at 1 atm P_{O_2}	Sensitivity (mbar)	Matrix	Reference
Ru(4,7)-Ph$_2$phen$_3{}^{2+}$	25	~37	RTV 118 silicone	[17]
[OS] (Ph$_2$phen)$_3$ Cl$_2$	~4.5	~289	PS 368.5	[27]
Platinum(II) octaethylporphyrin ketone (PtOEPK)	~20	~60	PS	[11]
Palladium(II) octaethylporphyrin ketone (PdOEPK)	>25	~0.92	PS	[11]
Erythrosin B	~123	0.016	Sol–gel silica	This work

[a] Sensitivity of an oxygen sensor is defined as the pressure of oxygen at which the phosphorescence intensity is euqal to $I_0/2$ [22].
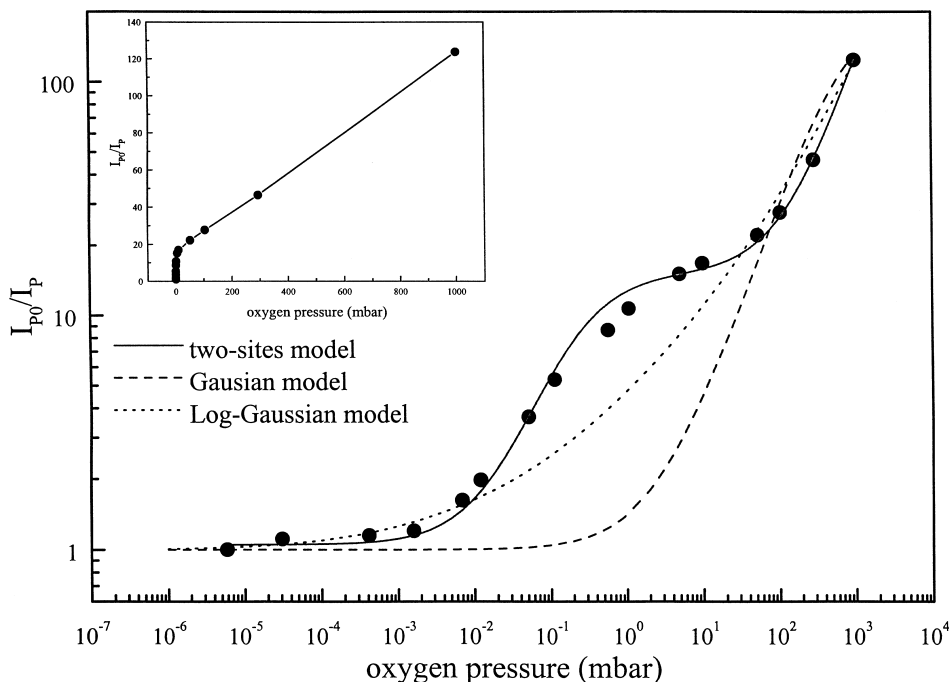
Fig. 2. SV plot and model fitting curves of phosphorescence intensity (I_P) in logarithmic scale and in linear scale (inset) for oxygen pressures from 10^{-6} to 1000 mbar.

The apparent good agreement between the experimental data and the two-site model predictions is not surprising since it is recognized that functions with two exponentials can yield excellent fits to complex decaying curves [18,19,22–24]. Although the two-site model may appear somewhat simplistic to accurately account for the complex process in a heterogeneous system, from a functional point of view, it allows for excellent mathematical prediction for calibration purposes. The variation of I as a function of P_{O_2} over wide pressure range can be predicted by the two-site model as long as I_0 and the value of P_{O_2} at which $I = I_0/2$ are known. The calibration process of the oxygen sensor is simplified. The value of the two-site model, therefore, lies in its simplicity.

To be consistent with intensity data that is successfully fitted by the two-site model, the decay time behavior data should follow a double exponential function with the decay time constants in agreement with the parameters derived from the intensity quenching data [8,16]. Decay of phosphorescence of the phosphorescence oxygen sensor was measured using a photo-multiplier in combination with a multi-channel scaler in the photon-counting configuration

[14]. Fig. 3 shows two typical decay curves at two different pressures. Both curves obey a double exponential function, suggesting that the decays are made up of two components. As in the case of many previous work [6–8,17,25], we experienced the same problem of consistency in modeling the decay lifetime data. To be consistent in modeling both the intensity data and the decay lifetime data, the value of f_1 in the intensity plot should be equal to that of α_1, the constant in the decay time exponential function (see Table 3). Values of α_1 varies from 0.2 to 0.79 over the P_{O_2} range of 3.4×10^{-6}–1.19 mbar whereas the value of f is 0.93 according to the SV plot.

Although the two-site model may not provide a complete description of the quenching behavior of the oxygen sensor, it does provide insights into the complex system. It implies there are at least two distinctly different environments within the erythrosin B sol–gel matrix, each being quenchable by oxygen but with different rate constants. It also appears that the decay kinetics of erythrosin B in sol–gel matrix is sufficiently complex that it defies explanations by simplistic models.

3.2. Temperature dependence

Significant temperature variations are frequently encountered in practical sensor applications. Compensations are necessary to correct for the deviations induced by temperature variation during measurement. A commonly employed method is to measure the temperature with a separate temperature sensor (for example a thermocouple) and correction is made to the luminescence intensity with a

Table 2
Model parameters

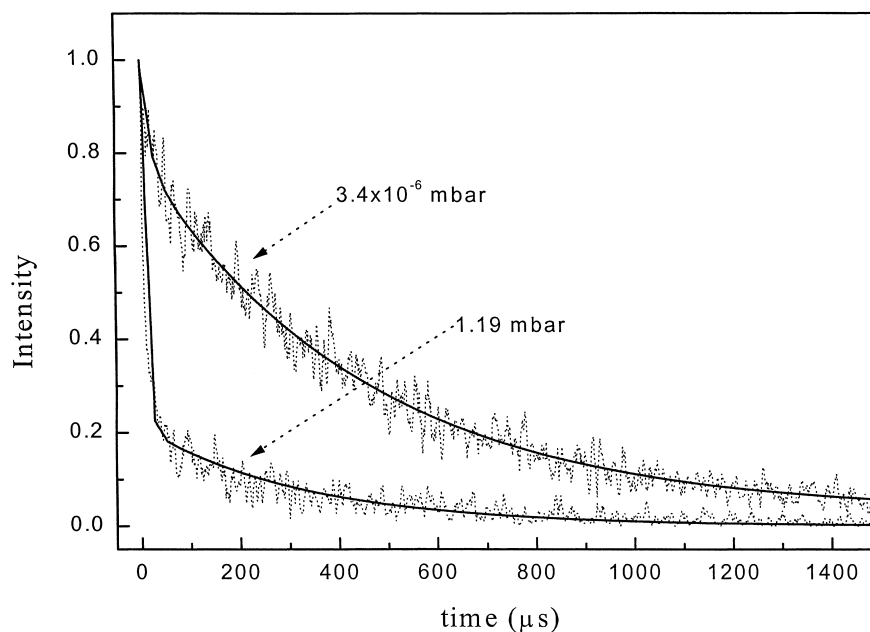| Two sites model	Gaussian model	Log-Gaussian model
$K_1 = 65 \pm 10 \text{ mbar}^{-1}$	$K_{av} = 0.43 \pm 0.17$ mbar^{-1}	$K_{av} = 30 \pm 20$ mbar^{-1}
$K_2 = 0.072 \pm 0.002 \text{ mbar}^{-1}$	$\rho = 0.62 \pm 0.07$	$\rho = 5.5 \pm 0.7$
$f = 0.930 \pm 0.002$		

Fig. 3. Lifetime decay curves of phosphorescence at pressures of 3.4×10^{-6} and 1.19 mbar, respectively.

pre-calibrated temperature response curve of the probe. Two sensors (one for oxygen and one for temperature), therefore, are needed for oxygen measurements to be rid of the temperature effect. For applications such as microanalysis where the local temperature under study could deviate considerably from the macro temperature (as monitored by the thermocouple for example), the two-probe method is no solution.

One of the characteristics of our phosphorescence oxygen sensor is that the luminescence spectra have two peaks as shown in Fig. 1. The small peak at short wavelength (570 nm) and the strong peak at long wavelength (691 nm) can be attributed to delayed fluorescence (DF) and phosphorescence (P) of erythrosin B, respectively. Both the phosphorescence and delayed fluorescence are quenched by oxygen (i.e. monotonical decrease of the intensity with oxygen pressure, see Fig. 2 or Fig. 5 of [13]). The responses of DF and P to temperature, however, indicate opposite behavior. Fig. 4a shows the delayed luminescence (both the phosphorescence and the delayed fluorescence) spectra at different temperatures. The phosphorescence intensity decreases as temperature increases. By contrast, the intensity of the delayed fluorescence is enhanced by the increase in temperature.

The opposite trends in the temperature dependence for phosphorescence and delayed fluorescence was observed in our earlier work [12,13]. The population of the energy

Table 3
Fitting parameters for time decay profiles at various oxygen pressures

	α_1	τ_1 (μs)	α_2	τ_1 (μs)
3.4×10^{-6} mbar	0.20	17.6	0.80	446
1.19 mbar	0.79	7.86	0.21	329

manifold of the lowest triplet state (T_1) follows a Maxwellian–Boltzmann distribution. More molecules occupy the higher vibrational/rotational sub-levels of the triplet state manifold (T_1) as temperature is increased. The rate of intersystem crossing from T_1 to the lowest excited singlet state S_1 also increases at higher temperature. As temperature increases, molecules originally residing in T_1 could populate S_1 via intersystem crossing, eventually ending up in the singlet ground state S_0 by radiative decay (delayed fluorescence). Hence, the intensity of delayed fluorescence gains at the expense of the phosphorescence at high temperature. The trend of delayed fluorescence is, therefore, opposite to that of phosphorescence as temperature varies. Fig. 4b shows this result with the intensity of both phosphorescence and delayed fluorescence normalized to that at room temperature at ambient pressure of 0.015 mbar.

By using this special property of temperature dependence, a self-compensation scheme of temperature can be developed for the oxygen sensor as the temperature dependence of the luminescence is independent of the oxygen pressure dependence. Temperature compensation can be done by monitoring the delayed fluorescence and phosphorescence simultaneously using the phosphorescence sensor probe. From the variation of the ratio of delayed fluorescence to phosphorescence, the temperature effect and the oxygen effect experienced by our sensor can be differentiated and then be corrected. From Fig. 4b, phosphorescence shows a continuous decay with increasing temperature whereas the change in delayed fluorescence is most drastic from −50 to 200°C. Therefore, this self-compensation scheme is most effective when the oxygen sensor operates within the temperature range from −50 to 200°C. Such self-contained temperature compensation removes the need of an
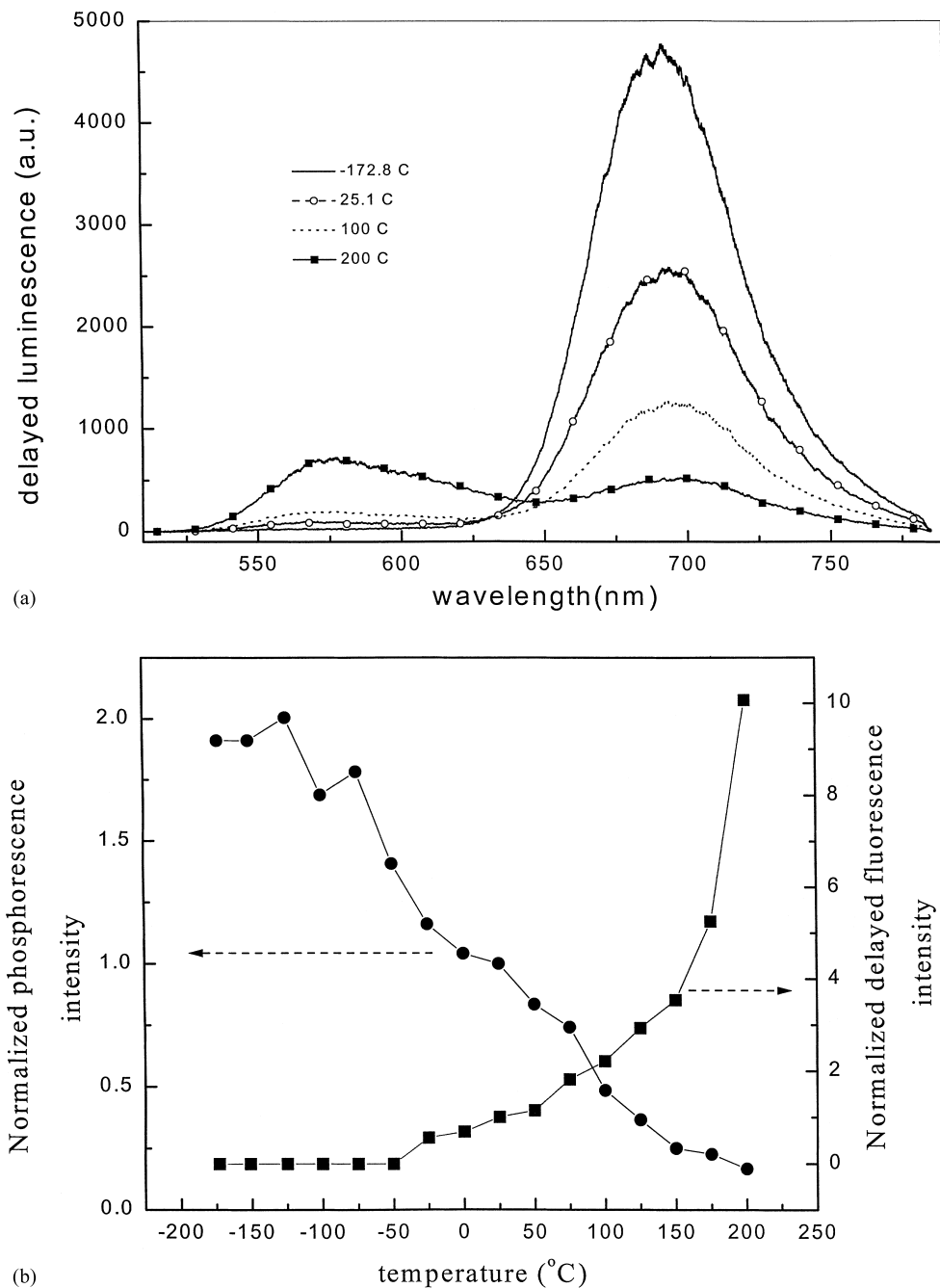
Fig. 4. (a) Delayed luminescence spectra at temperatures of −172.8, 25.1, 100 and 200°C, respectively. (b) Normalized (to the room temperature intensity) phosphorescence and delayed fluorescence intensity curves for the temperature range from −200 to 200°C.

additional temperature sensor and enables a more compact sensor design. We anticipate a wide range of applications of this self-compensated sensor especially in areas that require temperature measurements in the microscopic scale.

4. Conclusion

We have developed a phosphorescence-based oxygen sensor with erythrosin B doped sol–gel silica. Oxygen sensitivity of the probe is determined to be 0.012 mbar. The SV ratio is 10 times higher than that of most fluorescence-based oxygen sensor. The two-site model proves to be a superior fitting model for the nonlinear SV intensity curve. Although it may not fully describe the complicated kinetics processes in the heterogeneous sol–gel matrix, its usefulness lies in its simplicity. Temperature stability of the probe is also studied. Both phosphorescence and delayed fluorescence are found to be temperature sensitive but with opposite trend. By utilizing the ratio of

phosphorescence and delayed fluorescence to temperature variation, a sensor with self-compensation for temperature variation is possible.

Acknowledgements

References

[1] I. Kilmant, M. Kuhl, R.N. Glud, G. Holst, Sen. Actuators B 29 (1997) 38.
[2] B.D. MacCraith, C.M. McDonagh, G. O'Keeffe, A.K. McEvoy, T. Butler, F.R. Sheridan, Sens. Actuators B 29 (1995) 51.
[3] W. Trettnak, Optical sensors based on fluorescence quenching, in: O.S. Wolfbeis (Ed.), Fluorescence Spectroscopy, Springer, Berlin, 1992, p. 79.
[4] M. Lippitsch, J. Pusterhofer, M. Leiner, O. Wolfbeis, Anal. Chim. Acta 205 (1988) 1.
[5] W.W-S. Lee, K.Y. Wong, X.-M. Li, Anal. Chem. 65 (1993) 255.
[6] I. Kilmant, O.S. Wolfbeis, Anal. Chem. 67 (1995) 3160.
[7] H.N. McMurray, P. Douglas, C. Busa, M.S. Garley, J. Photochem. Photobiol. 80 (1994) 283.
[8] A. Mills, Analyst 124 (1999) 1301.
[9] S.-Y. Lee, I. Okura, Anal. Chim. Acta 342 (1997) 181.
[10] M.E. Diaz-Garcia, R. Pereiro-Garcia, N. Velasco-Garcia, Anal. Chem. 120 (1995) 457.
[11] P. Hartman, W. Trettnak, Anal. Chem. 68 (1996) 2615.
[12] S.K. Lam, D. Lo, Chem. Phys. Lett. 281 (1997) 35.
[13] S.K. Lam, E.B. Namdas, D. Lo, J. Photochem. Photobiol. A: Chem. 118 (1998) 25.
[14] M.A. Chan, J.L. Lawless, S.K. Lam, D. Lo, Anal. Chim. Acta 408 (2000) 33.
[15] W. Trettnak, W. Gruber, F. Reininger, L. Klimant, Sens. Actuators B 29 (1995) 219.
[16] A. Mills, A. Lepre, Anal. Chem. 69 (1997) 4653.
[17] E.R. Carraway, J.N. Demas, B.A. Degraff, J.R. Bacon, Anal. Chem. 63 (1991) 337.
[18] L. Sacksteder, J.N. Demas, B.A. Degraff, Anal. Chem. 65 (1993) 3480.
[19] E.R. Carraway, J.N. Demas, B.A. Degraff, J.R. Bacon, Anal. Chem. 63 (1991) 332.
[20] J.N. Demas, B.A. DeGraff, SPIE 1681 (1992) 2.
[21] J.N. Demas, B.A. DeGraff, Sens. Actuators B 29 (1995) 51.
[22] A. Mills, Sens. Actuators B 51 (1998) 69.
[23] D.R. James, Y.-S. Liu, P. DeMayo, W.R. Ware, Chem. Phys. Lett. 120 (1985) 460.
[24] A. Simiarczuk, W.R. Ware, J. Phy. Chem. 93 (1989) 7609.
[25] S. Draxler, M.E. Lippitsch, I. Kilmant, H. Kraus, O.S. Wolfbeis, J. Phy. Chem. 99 (1995) 3162.
[26] M.L. Bossi, M.E. Daraio, P.F. Aramendia, J. Photochem. Photobiol. A: Chem. 120 (1999) 15.
[27] W. Xu, K.A. Kneas, J.N. Demas, B.A. DeGraff, Anal. Chem. 68 (1996) 2605.

Biographies

M.A. Chan received BSEE degree from City College of New York in 1984. After graduation, she worked as a process engineer in Silicon Valley, USA. In 1990, she enrolled in the Biomedical Engineering program of University of California, Davis and received M.S. degree in 1992. She is currently performing research at the Chinese University of Hong Kong.

Sio Kuan Lam received his BSc degree in Applied Physics from Hua Chiao University, Fujien, China in 1990, MPhil degree in Applied Physics from the Hong Kong Polytechnic University, Hong Kong in 1995 and received his PhD degree in Physics from the Chinese University of Hong Kong, Hong Kong in 1998. He is currently a postdoctoral research fellow at the Chinese University of Hong Kong. His current research interests include dye-doped solid state laser based on sol–gel derived materials, fiber optical sensor for oxygen sensing, and nonlinear optical properties of organic dye doped sol–gel silica.

D. Lo received his B.S., M.S. and Ph.D. degrees from the Universities of California at Berkeley, Los Angeles and San Diego, respectively. His thesis research was on high current density and high-gas-pressure excimer lasers. From 1987 to 1992, he worked for Space Power Inc. in San Jose California on several novel laser projects funded by the United States Federal Government. Since 1993, he has been with the Physics Department, the Chinese University of Hong Kong. His current research interests are VUV laser development, sol–gel photonics and thermoluminescence dating of ancient ceramics.